Tunneling spin current in systems with spin degeneracy

Yuta Suzuki ●*

Department of Physics, The University of Tokyo, Bunkyo, Tokyo 113-0033, Japan

We study theoretically spin current generation from band insulators with PT symmetry, which is associated with Zener tunneling in strong dc electric fields. Each band in these systems is doubly degenerate with opposite spins, but spin rotational symmetry is not preserved in general. We consider the condition for spin current generation in connection with the nature of the wave function, which ultimately depends on a geometric quantity known as the shift vector. From an analysis of a two-band model, we find that the shift vector is necessary for spin current generation in PT-symmetric systems. We also present zigzag chain models that have shift vectors, and confirm from numerical calculations that a nonzero tunneling spin current occurs in spin-degenerate systems.

I. INTRODUCTION

Spin current generation by the application of an electric field has been extensively studied for crystals with various kinds of symmetries [1–3] and for the linear and nonlinear [4,5] response regimes. Even in nonmagnetic centrosymmetric crystals, it is possible to generate spin current provided spin rotational symmetry is broken by spin–orbit coupling (SOC). The intrinsic spin Hall effect [6] in metals and semiconductors is an example of this mechanism.

We can extend this idea to band insulators with both inversion and time-reversal symmetries. Here, spin current is associated with Zener tunneling [7] by a strong dc electric field. This tunneling is considered to be a nonadiabatic process, and the Landau–Zener formula [8–10] is useful for evaluating the tunneling probability of Bloch electrons across a band gap. In this formula, the tunneling probability is given by the electric field, band gap, and slope of the band dispersion. The tunneling spin current is then obtained from the difference in tunneling probabilities between two electrons with opposite spins [the definition is given in Eq. (10) below]. As mentioned above, spin current generation by an electric field is also allowed in the presence of SOC.

However, it is not obvious how a tunneling spin current arises in crystals with both inversion and time-reversal symmetries. This can be understood from the band dispersion: the combination of the space inversion and the time reversal operations, i.e., a PT operation, transforms the wave number k and spin σ that characterize the energy eigenvalues, as $(k, \sigma) \to (k, -\sigma)$, and each band is doubly degenerate with opposite spins, as shown in Fig. 1. Thus, focusing on the shape of the dispersions, it seems that the tunneling probabilities of two electrons with opposite spins are the same, and that no spin current is allowed in this system. The same consideration holds for insulators with PT symmetry that is invariant under the PT operation.

This naive estimate based on the band structure is, on the other hand, too restrictive for the spin current generation, compared to the results from the symmetry analysis. For 32 PT-symmetric point groups in 122 magnetic point groups [11], spin current can be associated with applied electric field in most cases, even in linear response regime; the tensor forms of spin Hall conductivity are listed in Ref. [[3], Table VII], where more than one component can remain finite even for PT-symmetric cases [12]. Thus, spin degeneracy in the band structure does not prevent spin current as a response to electric field, but its mechanism has not been identified for the Zener tunneling cas

We need to determine the origin of the tunneling spin current in a system with spin degeneracy. This is a challenge to the conventional idea that spin currents hardly arise in spin-degenerate crystals, and sheds light on the spin transport in these crystals.

The key to solving the problem is the nature of the wave function, rather than degenerate energy bands. Indeed, even in crystals with both global inversion and time-reversal symmetries, wave functions with opposite spins can be spatially shifted from each other [13,14]. In particular, it has recently been revealed that the geometric nature of the wave function is reflected in the tunneling process [5,15–17] and this effect can be reduced to a quantity called the *shift vector*, which is seen in the asymptotic formula of the tunneling probability [15,16]. The shift vector, known for the shift current in the photovoltaic effect [18–20], is a gauge-invariant quantity constructed from Berry connections of two bands. We expect that this quantity plays an important role in the nature of the tunneling phenomenon that cannot be explained from the band structure. One example that validates this idea is nonreciprocal tunneling in time-reversal systems [5,16].

In this paper, we consider tunneling spin current generation in PT-symmetric systems, in connection with the shift vector. Our discussion also applies to crystals with inversion and time-reversal symmetries.

This paper is organized as follows. In Sec. II, we show that it requires a nonzero shift vector to generate tunneling spin
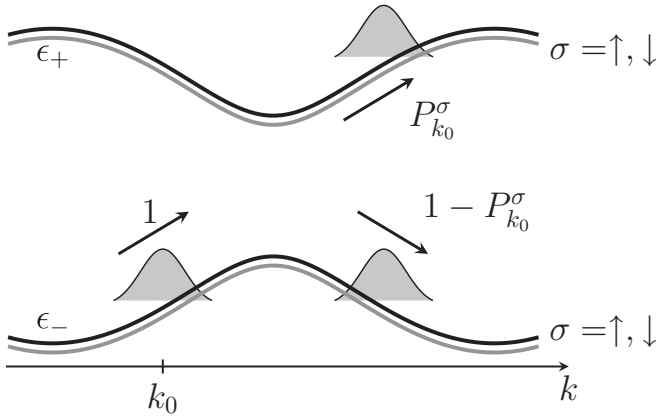
*suzuki@vortex.c.u-tokyo.ac.jp

FIG. 1. Schematic picture of the tunneling process in a system with spin degeneracy. When an electric field is applied, a wave packet characterized by wave number k_0 and spin σ tunnels from the valence band (ϵ_-) to the conduction band (ϵ_+) with probability $P_{k_0}^\sigma$.

current from the analysis of the time-dependent Schrödinger equation. In Sec. III, we confirm the generation of a tunneling spin current in a zigzag chain model with a finite shift vector, based on numerical calculations. The discussion in this section is generalized to a PT-symmetric system in Sec. IV. Finally, we provide a summary of our results and discuss how they can be generalized in Sec. V.

II. FORMULATION

A. Tunneling probability and current

We consider a one-dimensional lattice system with PT symmetry. First, we suppose that no external electric field is applied. For simplicity, we assume that a certain spin component $\hat{\sigma}$ is an exceptionally good quantum number of the system. Then, the Hamiltonian in crystal momentum space $\hat{H}(k)$ is described as follows:

$$\hat{H}(k) = \hat{H}^\uparrow(k) \oplus \hat{H}^\downarrow(k), \tag{1}$$

$$\hat{H}^\sigma(k)\big|u_n^\sigma(k)\big\rangle = \epsilon_n^\sigma(k)\big|u_n^\sigma(k)\big\rangle \tag{2}$$

where the symbols $\uparrow, \downarrow$ correspond, respectively, to the eigenvalues of the spin $\sigma = +1, -1$. As we have seen in Sec. I, PT symmetry leads to $\epsilon_n^\uparrow(k) = \epsilon_n^\downarrow(k) \equiv \epsilon_n(k)$ for any k. From now on, we focus on two gapped bands $n = \pm$ where $\epsilon_+(k) > \epsilon_-(k)$ holds.

We then consider a dc electric field E applied to this system from time $t = 0$. The Hamiltonian for $t > 0$ is obtained as $\hat{H}^\sigma(k - eEt/\hbar)$ in accordance with the Peierls substitution. (In this paper the charge of an electron is written as $-e$.) Suppose that the valence band $\epsilon_-^\sigma(k)$ is occupied and the conduction band ϵ_+^σ is empty for all k, σ. We take a wave number k_0 from the Brillouin zone (BZ) and define $|\Psi_{k_0}^\sigma(t)\rangle$ as the time evolution of a Bloch state in the valence band $|u_-^\sigma(k_0)\rangle$ from $t = 0$. This state satisfies the time-dependent Schrödinger equation

$$i\hbar\partial_t\big|\Psi_{k_0}^\sigma(t)\big\rangle = \hat{H}^\sigma(k_0(t))\big|\Psi_{k_0}^\sigma(t)\big\rangle \tag{3}$$

with $k_0(t) = k_0 - eEt/\hbar$, and the initial condition

$$\big|\Psi_{k_0}^\sigma(t = 0)\big\rangle = |u_-^\sigma(k_0)\rangle. \tag{4}$$

Now, we expand the state with snapshot eigenstates of $\hat{H}^\sigma(k_0(t))$ as

$$\big|\Psi_{k_0}^\sigma(t)\big\rangle = \sum_{n=\pm} a_{nk_0}^\sigma(t)e^{i\gamma_{nk_0}^\sigma(t)}\big|u_n^\sigma(k_0(t))\big\rangle. \tag{5}$$

Here, we introduced the coefficients $a_{\pm k_0}^\sigma$ and the sum of the dynamical phase and Berry phase

$$\gamma_{nk_0}^\sigma(t) = \int_{k_0}^{k_0(t)} dk \left[\frac{\epsilon_n(k)}{eE} + A_{nn}^\sigma(k) \right] \tag{6}$$

where the Berry connection $A_{nm}^\sigma(k) = \langle u_n^\sigma(k) | i\partial_k | u_m^\sigma(k)\rangle$ appears. Using these coefficients, the tunneling probability of the Bloch electron is defined as

$$P_{k_0}^\sigma(E, t) = \big|\langle u_+^\sigma(k_0(t)) | \Psi_{k_0}^\sigma(t)\rangle\big|^2 = \big|a_{+k_0}^\sigma(t)\big|^2. \tag{7}$$

We can also express the expectation value of the charge current $j^c = j^\uparrow + j^\downarrow$ and that of the spin current $j^s = \frac{\hbar}{2(-e)}(j^\uparrow - j^\downarrow)$ associated with the tunneling. As in the conventional way, j^σ is given as an expectation value of the velocity operator for all electrons in BZ, and is expressed as

$$j^\sigma(E, t) = \frac{-e}{L} \sum_{k_0 \in BZ} \big\langle \Psi_{k_0}^\sigma(t) | \hat{v}_{k_0}^\sigma(t) | \Psi_{k_0}^\sigma(t)\big\rangle. \tag{8}$$

Here, L is the system size and $\hat{v}_{k_0}^\sigma(t) = \frac{\partial \hat{H}^\sigma(k)}{\hbar \partial k}|_{k=k_0(t)}$ is the velocity operator. Note that this definition of the tunneling current is given in [5], where the effect of the fermionic heat bath is also considered in the expression.

If we take the limit $L \to \infty$ with periodic boundary conditions, we find the next expression (shown in Appendix A)

$$j^\sigma = \frac{-e}{\hbar} \int_{BZ} \frac{dk_0}{2\pi} \frac{\partial}{\partial k}\Big[\epsilon_{gap}(k)P_{k_0}^\sigma(k)\Big]\bigg|_{k=k_0(t)} \tag{9}$$

where we introduced $\epsilon_{gap} = \epsilon_+ - \epsilon_-$ and considered $P_{k_0}^\sigma(t)$ as a function of $k = k_0(t)$. In particular, the spin current is given as

$$j^s = \int_{BZ} \frac{dk_0}{2\pi} \frac{\partial}{\partial k}\left[\epsilon_{gap}(k)\frac{P_{k_0}^\uparrow(k) - P_{k_0}^\downarrow(k)}{2} \right]\Bigg|_{k=k_0(t)} \tag{10}$$

as mentioned in Sec. I.

B. Explicit expression for the time evolution

Substituting Eq. (5) into Eq. (3) gives

$$i\frac{\partial}{\partial t}a_{nk_0}^\sigma(t) = \frac{eE}{\hbar} \sum_{m(\neq n)} \big|A_{nm}^\sigma(k_0(t))\big|$$
$$e^{i\arg A_{nm}^\sigma(k_0)}e^{-i\Delta_{nm}^\sigma(k_0(t), k_0)}a_{mk_0}^\sigma(t) \tag{11}$$

where we introduced

$$\Delta_{nm}^\sigma(k, k_0) = \int_{k_0}^k dk' \frac{\epsilon_n(k') - \epsilon_m(k') + eER_{nm}^\sigma(k')}{eE}. \tag{12}$$

Here,

$$R_{nm}^\sigma(k) = A_{nn}^\sigma(k) - A_{mm}^\sigma(k) - \partial_k \arg A_{nm}^\sigma(k) \tag{13}$$

is called the *shift vector*.

As Eq. (4) gives $(a_{+k_0}^\sigma, a_{-k_0}^\sigma)|_{t=0} = (0, 1)$, we get a solution of Eq. (11) formally expressed as

$$\begin{pmatrix} a_{+k_0}^\sigma(t) e^{-i \arg A_{+-}^\sigma(k_0)} \\ a_{-k_0}^\sigma(t) \end{pmatrix} = \hat{T} \exp\left[i \int_0^t |A_{+-}^\sigma(k)| \begin{pmatrix} 0 & e^{-i\Delta_{+-}^\sigma(k,k_0)} \\ e^{+i\Delta_{+-}^\sigma(k,k_0)} & 0 \end{pmatrix}\Bigg|_{k=k_0(t')} \frac{-eE}{\hbar} dt' \right] \begin{pmatrix} 0 \\ 1 \end{pmatrix}. \quad (14)$$

Here, $\hat{T}$ is the time ordering operator. This formula shows that the information contained in the Hamiltonian is based on three quantities $\epsilon_{\text{gap}}(k)$, $|A_{+-}^\sigma(k)|$ and $R_{+-}^\sigma(k)$ that are all found to be gauge-invariant. Note that $R_{+-}^\sigma(k)$ is interpreted as being the difference in the intracell coordinate of the Bloch electron between the valence and conduction bands [21]. From this perspective, the spatial shift R_{+-}^σ yields the difference of the electrostatic potential between the two bands eER_{+-}^σ, which changes the energy to cross the band gap from ϵ_{gap} to $\epsilon_{\text{gap}} + eER_{+-}^\sigma$. We can find this term in Eq. (12). In real space, this effect appears as a correction to the depth of the tunnel barrier [16].

C. Origin of the spin dependence

The Berry connection and shift vector satisfy

$$|A_{+-}^\uparrow(k)| = |A_{+-}^\downarrow(k)|, \quad R_{+-}^\uparrow(k) = -R_{+-}^\downarrow(k) \quad (15)$$

in the PT-symmetric system. In a system with both inversion and time-reversal symmetries, as a special case of PT symmetry,

$$|A_{+-}^\sigma(-k)| = |A_{+-}^\sigma(+k)|, \quad R_{+-}^\sigma(-k) = -R_{+-}^\sigma(+k) \quad (16)$$

also holds for $\sigma = \uparrow, \downarrow$ in addition to Eq. (15). These derivations are given in Appendix B. Note that the shift vector remains finite in general even in such a highly symmetric system, though it vanishes if the system has spin rotational symmetry, in addition [16].

We now consider spin dependence of the tunneling probability in a PT-symmetric system. Equation (7) shows that the spin dependence results from the difference between $|a_{+k_0}^\uparrow|^2$ and $|a_{+k_0}^\downarrow|^2$. Here, the formula for $a_{nk_0}^\sigma$ is given in Eq. (14) and its spin dependence is reduced to that of $|A_{+-}^\sigma(k)|$ and $R_{+-}^\sigma(k)$ in $\Delta_{+-}^\sigma(k, k_0)$. In addition, $|A_{+-}^\sigma(k)|$ is spin-independent, as shown in Eqs. (15). Thus, the spin dependence of the tunneling probability is dependent only on the shift vector that changes its sign depending on its spin. We can also explain this result in terms of the energy to cross the band gap $\epsilon_{\text{gap}} + eER_{+-}^\sigma$. This energy is different between electrons with opposite spins, which leads to the difference in tunneling probability.

Furthermore, we can consider the condition of the spin current generation. If $R_{+-}^\sigma = 0$ holds, we then find that $P_{k_0}^\uparrow(t) = P_{k_0}^\downarrow(t)$ and $j^{\text{s}} = 0$ hold because of Eq. (10). This result implies that even in a system with spin degeneracy, tunneling spin current can be generated unless $R_{+-}^\sigma = 0$.

III. ZIGZAG CHAIN MODEL WITH BOTH INVERSION AND TIME-REVERSAL SYMMETRIES

In this section, we construct a simulation model with both inversion and time-reversal symmetries and derive a two-band Hamiltonian to show that tunneling spin current is induced by an electric field. Note that the model has previously been introduced in [[22], Sec. 7.2], except that a parameter v is added in the current study, as will be detailed later. In our model, we show that the shift vector remains finite since $v \neq 0$, and we confirm that the shift vector plays an important role in the spin current generation.

A. Tight-binding Hamiltonian

Let us consider a one-dimensional zigzag chain, shown in Fig. 2(a), with s, p orbitals at each atomic site. This chain belongs to the magnetic point group $2/m1'$, in other words, satisfies the following three conditions: (i) it has no magnetic orders and has time-reversal symmetry; (ii) it has inversion symmetry and the inversion center is located at the middle of the neighboring A and B sites; and (iii) it has reflection symmetry in a plane perpendicular to the z axis, while it breaks reflection symmetry in a plane perpendicular to the x
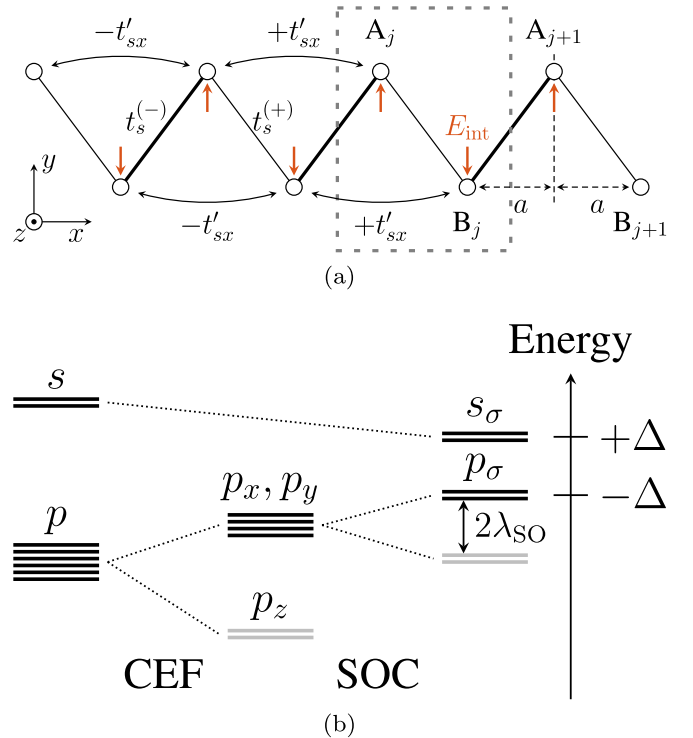

(a)

(b)

FIG. 2. Zigzag chain model and energy splitting diagram at each site. (a) The dashed gray rectangle shows a unit cell (jth), with two sublattices labeled A and B and lattice spacing a. The red vertical arrows denote a staggered internal electric field and the thick/thin solid lines denote nearest-neighbor hoppings (between two s orbitals), while the arcs denote next-nearest-neighbor hoppings (between s and p_x orbitals). (b) The degeneracy here includes the spin degree of freedom. CEF and SOC stand for crystalline electric field and spin–orbit coupling, respectively.

axis. We also introduce a crystalline electric field (CEF) that is consistent with the conditions above.

With the given symmetry of the system, we consider the Zener tunneling driven by an electric field E in the x direction, and tunneling spin current j^s that flows along the x direction with spin polarization along the z direction. This spin current component can be associated with the electric field unless the chain violates the three conditions above. Indeed, if the chain retains the reflection symmetry in a plane perpendicular to the x axis, which violates the condition (iii), the chain is symmetric under a two-fold rotation about the x axis, which keeps the electric field $E = E_x$ invariant but changes the sign of the spin current j^s. Then $j^s(E) = -j^s(E) = 0$ holds immediately. Thus, breaking of this reflection symmetry is essential for the existence of the tunneling spin current j^s. We will later use this property to verify our calculation in Sec. III B.

Based on the symmetry analysis above, we will construct a gapped two-band Hamiltonian of this chain, which corresponds to Eq. (1) with the spin quantization axis along the z direction. To begin with, we focus on the energy levels at each site as shown in Fig. 2(b). First, the CEF lifts the sixfold degenerate p orbitals into the energy levels (p_x, p_y) and p_z. Then, we consider the splitting of the p_x, p_y levels due to the SOC, which is given as $\hat{H}_{SO} = \lambda_{SO}\hat{l} \cdot \hat{\sigma}$. Here, $\hat{l}$ and $\hat{\sigma}$ are the orbital and spin angular momentum, respectively. We find that $\hat{l}_x, \hat{l}_y$ have no effect on the splitting because the p_x, p_y orbitals are related to the eigenstates of $\hat{l}_z$ through

$$|\pm 1\rangle \equiv |l = 1, m = \pm 1\rangle = \frac{1}{\sqrt{2}}(|p_x\rangle \pm i |p_y\rangle) \quad (17)$$

and $\langle \pm 1 | \hat{l}_{x,y} | \pm 1 \rangle = 0$ holds. Therefore, the term $\lambda_{SO}\hat{l}_z\hat{\sigma}_z$ lifts the degeneracy into two Kramers pairs, $(|+1, \uparrow\rangle, |-1, \downarrow\rangle)$ and $(|+1, \downarrow\rangle, |-1, \uparrow\rangle)$. We assume that the former pair

$$|p_\sigma\rangle \equiv \frac{1}{\sqrt{2}}(|p_x, \sigma\rangle + i\sigma |p_y, \sigma\rangle) \quad (\sigma = \sigma_z = \pm 1) \quad (18)$$

is at an energy level close to that of the s orbitals $|s_\sigma\rangle \equiv |s, \sigma\rangle$, as shown in Fig. 2(b). For simplicity, we take the energy levels of $|s_\sigma\rangle, |p_\sigma\rangle$ to be $+\Delta, -\Delta$.

We then focus on the on-site parity mixing due to the internal electric field as shown in Fig. 2(a), which appears when the inversion center is not located at a site. To see this, we introduce the local electrostatic potential $\hat{V}_{in}$ as follows:

$$\hat{V}_{in}(y) = \begin{cases} -E_{in}y & \text{near A sites} \\ +E_{in}y & \text{near B sites} \end{cases} \quad (19)$$

where the inversion center is placed at $y = 0$. Here, $\hat{V}_{in}$ satisfies the global inversion symmetry and meets the conditions (i)–(iii). Then, the mixing $\langle s | (-e)\hat{V}_{in} | p_y \rangle$ occurs at each site and we find from Eq. (18) that

$$\langle s_{\sigma A}|(-e)\hat{V}_{in}|p_{\sigma A}\rangle = -\langle s_{\sigma B}|(-e)\hat{V}_{in}|p_{\sigma B}\rangle = i\sigma\phi. \quad (20)$$

Here, we introduced a constant ϕ.

We also introduce the transfer integrals $t_s^{(\pm)}$ and t'_{sx} as shown in Fig. 2(a). The signs with t'_{sx} are determined by the direction dependence of $|s\rangle, |p_x\rangle$. It is also natural to assume that $t_s^{(+)}$ and $t_s^{(-)}$ have the same sign in this model.

Thus, we get the tight-binding Hamiltonian

$$\hat{\mathcal{H}}^{s-p} = \sum_{j,\sigma,\tau} \Delta(\hat{s}_{j\tau\sigma}^\dagger \hat{s}_{j\tau\sigma} - \hat{p}_{j\tau\sigma}^\dagger \hat{p}_{j\tau\sigma})$$

$$+ \sum_{j,\sigma} (i\sigma\phi)(\hat{s}_{jA\sigma}^\dagger \hat{p}_{jA\sigma} - \hat{s}_{jB\sigma}^\dagger \hat{p}_{jB\sigma})$$

$$+ \sum_{j,\sigma} (t_s^{(+)}\hat{s}_{jA\sigma}^\dagger \hat{s}_{j,B\sigma} + t_s^{(-)}\hat{s}_{jA\sigma}^\dagger \hat{s}_{j-1,B\sigma})$$

$$+ \sum_{j,\sigma,\tau} t'_{sx}(\hat{s}_{j\tau\sigma}^\dagger \hat{p}_{j+1,\tau\sigma} - \hat{s}_{j\tau\sigma}^\dagger \hat{p}_{j-1,\tau\sigma}) + \text{H.c.} \quad (21)$$

where $\hat{s}_{j\tau\sigma}^\dagger, \hat{s}_{j\tau\sigma}, \hat{p}_{j\tau\sigma}^\dagger, \hat{p}_{j\tau\sigma}$ are electron creation and annihilation operators on the jth site, labeled with orbital (s, p), spin $(\sigma = \uparrow, \downarrow)$ and sublattice $(\tau = A, B)$.

In the crystal momentum space, the Hamiltonian is expressed as follows:

$$\hat{\mathcal{H}}^{s-p} = \sum_{k\sigma} \hat{C}_{k\sigma}^\dagger H_{k\sigma}^{s-p} \hat{C}_{k\sigma}, \quad (22)$$

$$H_{k\sigma}^{s-p} = \begin{pmatrix} \Delta & \alpha_k & \beta_{k\sigma}^{(+)} & 0 \\ \alpha_k^* & \Delta & 0 & \beta_{k\sigma}^{(-)} \\ \beta_{k\sigma}^{(+)*} & 0 & -\Delta & 0 \\ 0 & \beta_{k\sigma}^{(-)*} & 0 & -\Delta \end{pmatrix}. \quad (23)$$

Here, we introduced

$$\alpha_k = t_s^{(+)}e^{+ika} + t_s^{(-)}e^{-ika}, \quad \beta_{k\sigma}^{(\pm)} = 2it'_{sx}\sin(2ka) \pm i\phi\sigma \quad (24)$$

and $\hat{C}_{k\sigma}^\dagger = (\hat{s}_{kA\sigma}^\dagger, \hat{s}_{kB\sigma}^\dagger, \hat{p}_{kA\sigma}^\dagger, \hat{p}_{kB\sigma}^\dagger)$ obtained from the Fourier transformation of $\hat{s}_{j\tau\sigma}^\dagger, \hat{p}_{j\tau\sigma}^\dagger$. Let us now assume that $\phi, t_s^{(\pm)}, t'_{sx} \ll \Delta$ and derive the effective Hamiltonian for $|s_\sigma\rangle$. We divide 4×4 matrix $H_{k\sigma}^{s-p}$ into 2×2 blocks as

$$H_{k\sigma}^{s-p} = \begin{pmatrix} H_{k\sigma}^s & H_{k\sigma}^1 \\ H_{k\sigma}^{1\dagger} & H_{k\sigma}^p \end{pmatrix} \quad (25)$$

and obtain the effective Hamiltonian

$$\tilde{H}_{k\sigma}^s \simeq H_{k\sigma}^s + \frac{1}{2\Delta}H_{k\sigma}^1 H_{k\sigma}^{1\dagger} = H^\sigma(k) + \text{(scalar)} \quad (26)$$

where we can neglect the scalar term since it has no effect on the tunneling process. We find that

$$H^\sigma(k) = \begin{pmatrix} -u\sigma \sin(ka)\cos(ka) & w\cos(ka) - iv\sin(ka) \\ w\cos(ka) + iv\sin(ka) & u\sigma \sin(ka)\cos(ka) \end{pmatrix}$$

$$= \boldsymbol{d}^\sigma(k) \cdot \boldsymbol{\tau} \quad (27)$$

with Pauli matrices $\boldsymbol{\tau} = (\tau_x, \tau_y, \tau_z)$. This two-band Hamiltonian is characterized by the following:

$$u = \frac{-4t'_{sx}\phi}{\Delta}, \quad v = t_s^{(-)} - t_s^{(+)}, \quad w = t_s^{(+)} + t_s^{(-)}, \quad (28)$$

$$\boldsymbol{d}^\sigma(k) = (w\cos(ka), v\sin(ka), -\sigma u\sin(ka)\cos(ka)). \quad (29)$$

Let us examine each component of $\boldsymbol{d}^\sigma(k)$. The first component always remains finite since $t_s^{(+)}$ and $t_s^{(-)}$ have the same sign, as mentioned above. The second component with v, however, disappears if the model recovers reflection symmetry in a plane perpendicular to the x axis, since $t_s^{(+)} = t_s^{(-)}$ holds in this case. Thus, we can consider this component to
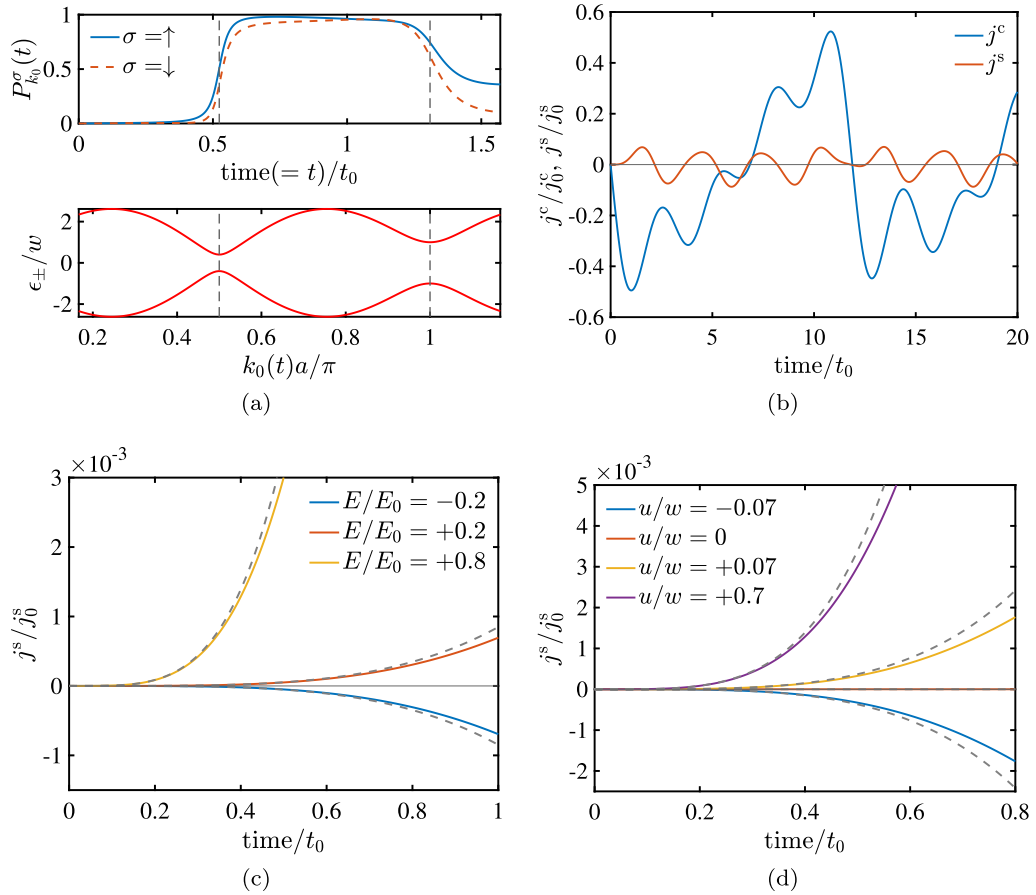
FIG. 3. Numerical results for time variation of tunneling probability and charge/spin current in the zigzag chain model with both inversion and time-reversal symmetries. (a) Tunneling probability (upper row) across the energy levels (lower row) with the parameters $(k_0 a, u/w, v/w, E/E_0) = (\pi/6, 5, 0.4, -2)$. The dashed vertical lines show where the band gap is locally minimum. (b) Charge and spin currents with the parameters $(u/w, v/w, E/E_0) = (0.7, 0.4, 0.8)$. (c) Electric field dependence of the spin current shortly after application of electric field with the parameters $(u/w, v/w) = (0.7, 0.4)$. The dashed curves represent $j^s(E, t)$ from the analytical formula (32). (d) Spin current shortly after the application of an electric field for different values of antisymmetric SOC parameter u, with the parameters $(v/w, E/E_0) = (0.4, 0.8)$. The dashed curves represent $j^s(E, t)$ from the analytical formula (32).

be the result of reflection symmetry breaking. We also find that the third component of $\boldsymbol{d}^\sigma(k)$ emerges due to the lack of local inversion symmetry, since $\phi = 0$ holds if an inversion center can be placed at each lattice site. This term is known as the antisymmetric spin–orbit interaction in lattice structures such as zigzag [23,24], honeycomb and diamond structure, which are all globally centrosymmetric systems but break the inversion symmetry at lattice sites [25]. Note that it is easy to see that this component corresponds to SOC when the SOC splitting is small enough to satisfy $\lambda_{SO} \ll \Delta$. In this case, we should take into account the additional energy level just below $|p_\sigma\rangle$ shown in Fig. 2(b). The parameter u is then modulated as

$$u = \frac{-4t'_{sx}\phi}{\Delta} \rightarrow -4t'_{sx}\phi\left(\frac{1}{\Delta} - \frac{1}{\Delta + \lambda_{SO}}\right) \simeq \frac{-4t'_{sx}\phi\lambda_{SO}}{\Delta^2} \tag{30}$$

and is indeed proportional to λ_{SO}.

Now, we check if the shift vector in this model remains finite. From the Hamiltonian (27), we can express it as

follows:

$$R^\sigma_{+-}(k)$$
$$= \frac{(\boldsymbol{d}^\sigma \times \partial_k \boldsymbol{d}^\sigma) \cdot (\partial_k^2 \boldsymbol{d}^\sigma)}{(\boldsymbol{d}^\sigma \times \partial_k \boldsymbol{d}^\sigma)^2}\sqrt{(\boldsymbol{d}^\sigma)^2}$$
$$= \frac{3}{2}uvw\sin(2k)\frac{\sqrt{u^2\sin^2 k\cos^2 k + v^2\sin^2 k + w^2\cos^2 k}}{v^2 w^2 + u^2 w^2\cos^6 k + u^2 v^2\sin^6 k}\sigma \tag{31}$$

where we used the formula given in [16] and take $a = 1$. Equation (31) shows that $R^\sigma_{+-}(k) \neq 0$ holds when $u, v, w \neq 0$.

B. Numerical calculations

From the Hamiltonian (27), the behaviors of $P^\sigma_{k_0}(t)$, $j^c(E, t)$, and $j^s(E, t)$ are obtained numerically as shown in Fig. 3. Here, we introduced $t_0 = \hbar/w$, $E_0 = w/(ea)$, $j^c_0 = (-e)w/\hbar$, and $j^s_0 = w/2$ as a typical time length, electric field, charge current, and spin current, respectively.

In Fig. 3(a), we can see that the probabilities with opposite spins are different from each other, which is expected since

$u \neq 0$ breaks spin rotational symmetry in our model. Note that $P_{k_0}^{\sigma}(t)$ has a steep rise and fall in the vicinity of $k = k_0(t)$ where the band gap is locally minimum. This behavior is characteristic of tunneling. We also find from Fig. 3(b) that a nonzero spin current is associated with an electric field in this model. This spin current generation purely originates from a nonzero shift vector, i.e., the geometric effect of the wave function, since each band is doubly degenerate with opposite spins.

Figure 3(b) also shows an oscillating behavior in the charge and spin currents, the reason for which can be explained as follows: the Hamiltonian of this model $\hat{H}^{\sigma}(k_0(t))$ is time-periodic with period $T \equiv 2\pi\hbar/(e|E|a)$, and we can consider that the Schrödinger equation (3) describes a kind of Rabi cycle driven by an external field with period T. Thus, we see an oscillation in the population $|a_{nk_0}^{\sigma}(t)|^2$ and that of the currents $j^s(t)$. For more details, see Appendix C. Here, T corresponds to the period of the Bloch oscillation, though it is hard to observe the oscillation in experiments since T is large. Thus, we focus on the time period shortly after application of the electric field, i.e., $t \ll t_0$.

In this region, the tunneling spin current can be approximated as

$$
\begin{aligned}
& j^s(E, t)/j_0^s \\
& \simeq \frac{-5}{12\pi} \left(\frac{1}{a^3 w^2} \int_{\text{BZ}} dk \epsilon_{\text{gap}} (\partial_k \epsilon_{\text{gap}}) |A_{+-}^{\uparrow}|^2 R_{+-}^{\uparrow} \right) \\
& \quad \left(\frac{E}{E_0} \right)^3 \left(\frac{t}{t_0} \right)^4,
\end{aligned} \tag{32}
$$

and is scaled by the integral containing the shift vector $R_{+-}^{\uparrow}$. This expression is derived in Appendix D. In Fig. 3(c), this formula fits the numerically obtained $j^s(t)$ for each value of E/E_0. The relation $j^s(-E) = -j^s(+E)$ also holds in both Fig. 3(c) and Eq. (32), which is expected from the inversion symmetry of the model.

As we mentioned in Sec. II C, this spin current disappears when the shift vector goes to zero. This means that $j^s = 0$ holds if the antisymmetric SOC vanishes ($u = 0$) or the reflection symmetry is restored ($v = 0$) in our zigzag chain model. The curve of $u = 0$ in Fig. 3(d) demonstrates this behavior. Moreover, Fig. 3(d) shows a trend of the spin current increasing as u moves away from zero. In the Supplemental Material [26], we check that the same trend holds for the parameter v. Note that this relation between $j^s = 0$ and the existence of reflection symmetry $v = 0$ is consistent with the symmetry analysis as mentioned in Sec. III A. These results and the integral in Eq. (32) indicate that as long as u, v are small enough, the shift vector is increased by the antisymmetric SOC and reflection symmetry breaking, which enhances the tunneling spin current in the zigzag chain model.

IV. GENERAL ZIGZAG CHAIN MODEL WITH PT SYMMETRY

We now generalize the zigzag chain model in Sec. III by introducing staggered magnetic order on each site. In this model, illustrated in Fig. 4(a), the magnetic point group is given as $2'/m$ where inversion and time-reversal symmetries

are both broken, but PT symmetry is preserved. Introducing the magnetic order may seem to be artificial, but it is known that for a zigzag chain model, which has itinerant electrons and localized spins, the staggered antiferromagnetic order along the chain is stabilized near half filling [27].

Now, the molecular field from the magnetic order is expressed as

$$
\hat{\mathcal{H}}_{\text{AF}} = \sum_{k\sigma} \hat{C}_{k\sigma}^{\dagger} \begin{pmatrix} \phi_s \sigma & & & \\ & -\phi_s \sigma & & \\ & & \phi_s \sigma & \\ & & & -\phi_s \sigma \end{pmatrix} \hat{C}_{k\sigma}. \tag{33}
$$

We add this term to the Hamiltonian (22) and derive the effective Hamiltonian $H^{\sigma}(k)$ for $|s_{\sigma}\rangle$ in the same way as in Sec. III. Then, we obtain

$$
H^{\sigma}(k) = \tilde{\boldsymbol{d}}^{\sigma}(k) \cdot \boldsymbol{\tau} \tag{34}
$$

with

$$
\tilde{\boldsymbol{d}}^{\sigma}(k) = (w\cos(ka), v\sin(ka), \sigma[\phi_s - u\sin(ka)\cos(ka)]) \tag{35}
$$

where u, v, w are the same as those defined in Eq. (28).

In this model, the expression for the shift vector is rather complicated, and we focus on whether a spin current can be generated from this model. Figure 4(b) plots charge and spin currents computed from the Hamiltonian (34). The nonzero spin current shown here ensures that tunneling spin current occurs even in insulators with spin degeneracy by the application of an electric field. Again, oscillating behaviors of the charge and spin currents are evident, and we give the reason for this in Appendix C.

Let us focus on the time period shortly after the application of the electric field. Then, the tunneling spin current from this model is approximated as

$$
\begin{aligned}
& j^s(E, t)/j_0^s \\
& \simeq \frac{2}{3\pi} \left(\frac{1}{a^2 w^2} \int_{\text{BZ}} dk \epsilon_{\text{gap}}^2 |A_{+-}^{\uparrow}|^2 R_{+-}^{\uparrow} \right) \left(\frac{E}{E_0} \right)^2 \left(\frac{t}{t_0} \right)^3 \tag{36}
\end{aligned}
$$

in the PT-symmetric model. We derive this expression in Appendix D. In Fig. 4(c), this formula fits the behavior of $j^s(t)$ for each value of E/E_0. We also find from Fig. 4(c) that this spin current satisfies nonreciprocity, i.e., the relation $j^s(-E) \neq -j^s(+E)$, which is expected from the lack of inversion symmetry in this model.

V. DISCUSSION AND CONCLUSIONS

We investigated whether a tunneling spin current is induced by an electric field in connection with the shift vector. We focused on a system with PT symmetry but without spin rotational symmetry, including a system with both inversion and time-reversal symmetries. First, we find from the analytic calculations for a two-band model in Sec. II that a shift vector is necessary for spin current generation. Then, in Sec. III, we demonstrate a model that has a shift vector and calculated the spin current numerically. We confirm that even in a system with inversion and time-reversal symmetries, a spin current can be generated because of the shift vector. We extend this discussion to the general PT-symmetric system, where tunneling spin current also arises, in Sec. IV.
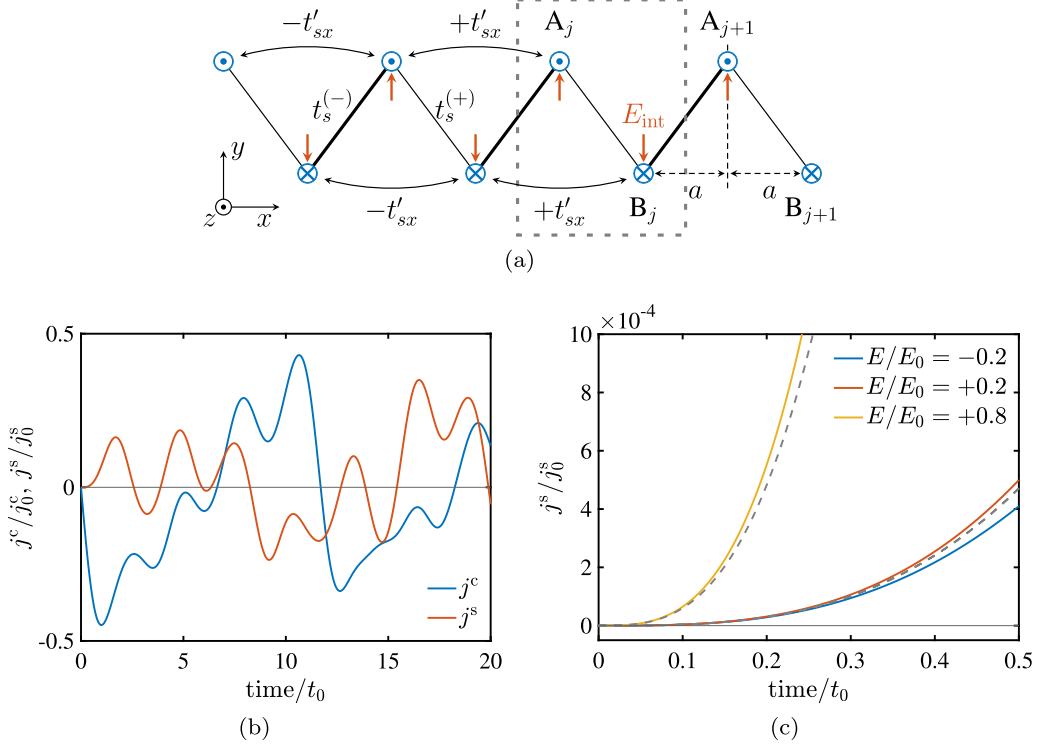
FIG. 4. Generalized model with PT symmetry and numerical results for tunneling charge/spin current from this model. (a) Zigzag chain model with PT symmetry. The components in the model are the same as those in Fig. 2(a), except for the staggered magnetic order on each site (shown as blue circles ⊙, ⊗). (b) Time variations of charge and spin currents in the zigzag chain model with PT symmetry. We used the parameters $(u/w, v/w, \phi_s/w, E/E_0) = (0.7, 0.4, 0.2, 0.8)$. (c) Electric field dependence of the spin current shortly after the application of an electric field. The dashed curves represent $j^s(E, t)$ from the analytical formula (36). We used the parameters $(u/w, v/w, \phi_s/w) = (0.7, 0.4, 0.2)$.

To summarize, we have exactly identified the microscopic origin of the spin current in PT-symmetric insulators, associated with Zener tunneling; that is shift vector, a purely geometric quantity, which yields the spin-dependent tunneling process in the spin-degenerate system. Since our analysis in Sec. II is not limited to specific systems, this result holds for any one-dimensional PT-symmetric insulators where we can neglect both spin flip in the tunneling process and transitions from/to other states than the valence and conduction bands.

Indeed, there are some other recent works on the Zener tunneling that examined the geometric effect on it. In particular, the authors of Refs. [5,16] made it clear that the shift vector corrects the charge/spin transport calculated from the band structure. However, they considered time-reversal symmetric but noncentrosymmetric insulators, not the PT-symmetric ones. Also, they focused on nonreciprocity of the transport due to the shift vector, not on the spin current generation itself. Thus, it is unique to our paper that the Zener tunneling in PT-symmetric insulators is studied, and that the relation between the spin current generation and the shift vector are clarified.

We can summarize this paper from a different point of view. In the beginning of Sec. III A, we have discussed the symmetry requirement for the zigzag chain model to have a nonzero tunneling spin current. Such symmetry analysis offers a qualitative approach to estimate such nonlinear spin current response. On the other hand, we have described the

mechanism of the tunneling spin current in Sec II, which offers a quantitative approach. We can evaluate the spin current based on the approximated formula such as Eq. (32) or (36) which depends on the shift vector. We can make use of both such qualitative and quantitative evaluations provided in this paper to design or to search for insulators with a relatively large tunneling spin current.

Now, we would like to refer to how our results can be generalized. We have so far considered the spin current associated with dc electric field in one-dimensional two-band PT-symmetric insulators where spin in a certain direction is conserved. We will first describe how to extend our analysis to two- or three-dimensional insulators. Next, we will consider the case when an ac electric field, instead of dc one, is applied to the system. At the end, we will discuss the implications of our results for multi-band systems, non-PT-symmetric systems, and systems where spin is no longer a conserved quantity.

First, we can apply our results obtained in one-dimensional lattice systems to two- or three-dimensional ones. In these systems, the Bloch electron with wave vector $\boldsymbol{k}$ at the time $t = 0$ is driven by the field to have $\boldsymbol{k} - e\boldsymbol{E}t/\hbar = (\boldsymbol{k}_\perp, k_\parallel - eEt/\hbar)$, where $\boldsymbol{k}_\perp$, $k_\parallel$ is the component perpendicular, parallel to the external electric field $\boldsymbol{E}$, respectively. We then slice the crystal momentum space into one-dimensional ones along the electric filed, labeled with different $\boldsymbol{k}_\perp$. The Zener tunneling takes place in each slice [28]. We find that the Hamiltonian of each slice is still PT symmetric, and can define tunneling probabil-

ity, spin current, and shift vector of each slice as the same way as in Sec. II. Thus, as we have found in the one-dimensional lattice systems, the shift vector plays an important role in the spin current generation even in the two- or three-dimensional systems.

It is also interesting to consider the spin current as a response to ac electric field from the same PT-symmetric system. It is known that tunneling, as a response to a strong dc electric field, undergoes a crossover in response to a weak ac electric field in the plane of the field strength and frequency [[29], Sec. IIIA]. For example, in noncentrosymmetric crystals, there are known two effects both caused by shift vectors, namely shift current [18–20] and nonreciprocal Zener tunneling [5,16] in ac and dc responses, respectively. In the same way, as a counterpart of the tunneling spin current we studied here, there is a mechanism of shift spin current driven by ac electric field in PT-symmetric insulators, which has been listed in Ref. [[30], Table 2].

Returning to the case of the Zener tunneling under dc electric field, our results has importance even when more than two bands are involved in the non-adiabatic transitions, when PT symmetry is broken, or when spin is no longer conserved. In these systems, two-level transition picture is no longer valid, and we have to consider the multilevel transitions of electrons from occupied bands and the Pauli exclusion principle between them. Then, the time evolution of a Bloch electron under the driving field is described with field operators [5,28] as $\hat{c}_\alpha(k_0) \rightarrow \sum_\beta a_{\beta k_0}(t) e^{i\gamma_{\beta k_0}(t)} \hat{c}_\beta(k_0(t))$. Here, α, β are band indices and $\gamma_{\beta k_0}(t)$ is a sum of the dynamical phase and Berry phase, defined similarly to Eq. (6). The coefficients $a_{\beta k_0}(t)$ also obeys a similar equation as Eq. (11) in which expression shift vector $R_{\alpha\beta}$ is included and modulates the energy to cross the band gap from $\epsilon_\alpha - \epsilon_\beta$ to $\epsilon_\alpha - \epsilon_\beta + eER_{\alpha\beta}$. As a result, the shift vector contributes to the tunneling process even in these systems. In particular, the shift vector is spin-dependent quantity even in spin-degenerate systems, as we have seen. Thus, the shift vector still provides a substantial contribution to the spin-dependent Zener tunneling in many insulators.

This idea to examine spin current in connection with the shift vector may be important to explain the outstanding spin dependent transport in some chiral molecules. Recent experiments have revealed that the chiral molecules make electrons transmitted through themselves spin polarized without magnetic fields, which is referred to as chirality-induced spin selectivity (CISS) effect [31,32]. However, microscopic theory of this spin filter effect is still under debate [33]. One approach to this problem is to assume that the transport is electron tunneling, and to analyze the spin-dependent tunneling process in such chiral structures [5]. In this way, the geometric contribution to the tunneling spin current that is stressed here may provide hints for the unexplained spin transport in the chiral molecules.

APPENDIX A: EXPRESSION FOR THE TUNNELING CURRENT

Here, we derive Eq. (9) from the definition (8). First, we find from the Schrödinger equation (3) that

$$
\frac{\partial}{\partial t} \langle \Psi^\sigma_{k_0}(t) | \hat{H}^\sigma(k_0(t)) | \Psi^\sigma_{k_0}(t) \rangle
$$

$$
= \langle \Psi^\sigma_{k_0}(t) | \hat{H}^\sigma(k_0(t)) | \partial_t \Psi^\sigma_{k_0}(t) \rangle + \text{c.c.}
$$

$$
+ \langle \Psi^\sigma_{k_0}(t) | \frac{\partial \hat{H}^\sigma(k_0(t))}{\partial t} | \Psi^\sigma_{k_0}(t) \rangle \tag{A1}
$$

$$
= \frac{1}{i\hbar} \langle \Psi^\sigma_{k_0}(t) | \left[\hat{H}(k_0(t)) \right]^2 | \Psi^\sigma_{k_0}(t) \rangle + \text{c.c.}
$$

$$
+ \frac{\partial k_0(t)}{\partial t} \langle \Psi^\sigma_{k_0}(t) | \frac{\partial \hat{H}^\sigma(k)}{\partial k} \bigg|_{k=k_0(t)} | \Psi^\sigma_{k_0}(t) \rangle \tag{A2}
$$

$$
= -eE \langle \Psi^\sigma_{k_0}(t) | \hat{v}^\sigma_{k_0}(t) | \Psi^\sigma_{k_0}(t) \rangle \tag{A3}
$$

where $\hat{v}^\sigma_{k_0}(t)$ is the velocity operator introduced in Sec. II A.

Then, Eq. (5) leads to

$$
\langle \Psi^\sigma_{k_0}(t) | \hat{H}^\sigma(k_0(t)) | \Psi^\sigma_{k_0}(t) \rangle
$$

$$
= \epsilon_+(k_0(t)) \left| a^\sigma_{+k_0}(t) \right|^2 + \epsilon_-(k_0(t)) \left| a^\sigma_{-k_0}(t) \right|^2 \tag{A4}
$$

$$
= \epsilon_{\text{gap}}(k_0(t)) P^\sigma_{k_0}(t) + \epsilon_-(k_0(t)), \tag{A5}
$$

using the conservation of probability $\langle \Psi^\sigma_{k_0}(t) | \Psi^\sigma_{k_0}(t) \rangle = |a^\sigma_{+k_0}(t)|^2 + |a^\sigma_{-k_0}(t)|^2 = 1$. Finally, combining Eq. (A3) and Eq. (A5), we have

$$
-e \langle \Psi^\sigma_{k_0}(t) | \hat{v}^\sigma_{k_0}(t) | \Psi^\sigma_{k_0}(t) \rangle
$$

$$
= \frac{1}{E} \frac{\partial}{\partial t} \left[\epsilon_{\text{gap}}(k_0(t)) P^\sigma_{k_0}(t) \right] + \frac{1}{E} \frac{\partial \epsilon_-(k_0(t))}{\partial t}. \tag{A6}
$$

We then integrate both sides of Eq. (A6) over the BZ. The second term in the right-hand side of Eq. (A6) vanishes and we obtain Eq. (9).

APPENDIX B: SYMMETRY CONSIDERATIONS OF THE BERRY CONNECTION AND SHIFT VECTOR

In this Appendix, we consider the symmetry of the Berry connection and shift vector reflecting the discrete symmetry of the spinful system. Note that the case when the system has spin rotational symmetry is considered in [16]. Let us focus on a system that is invariant under a discrete transformation, such as space inversion $\hat{\Pi}$, time-reversal $\hat{\Theta}$, or PT transformation $\hat{\Pi}\hat{\Theta}$. The Hamiltonian of this system satisfies

$$
\hat{O} \hat{H}(k) = \hat{H}(\chi k) \hat{O} \tag{B1}
$$

with $(\hat{O}, \chi) = (\hat{\Pi}, -1), (\hat{\Theta}, -1), (\hat{\Pi}\hat{\Theta}, +1)$.

The eigenstates of the Hamiltonian are introduced as $\hat{H}(k) |u_\alpha(k)\rangle = \epsilon_\alpha(k) |u_\alpha(k)\rangle$ where $\alpha = (n, \sigma)$ is a combination of band and spin indices. We then find from Eq. (B1) that $\hat{O} |u_\alpha(k)\rangle$ is one of the eigenstates of $\hat{H}(\chi k)$ with energy $\epsilon_\alpha(k)$. We consider this state labeled with another band index

$\tilde{\alpha}$ such that

$$|u_{\tilde{\alpha}}(\chi k)\rangle = e^{-i\theta_\alpha(k)}\hat{O}|u_\alpha(k)\rangle, \quad \epsilon_{\tilde{\alpha}}(\chi k) = \epsilon_\alpha(k) \quad \text{(B2)}$$

where the difference in the phase $\theta_\alpha(k)$ remains in general.

From the definition of the Berry connection and Eq. (B2), we find that

$$A_{\tilde{\alpha}\tilde{\beta}}(\chi k) = \langle u_{\tilde{\alpha}}(\chi k) | i\partial_{\chi k} | u_{\tilde{\beta}}(\chi k)\rangle \quad \text{(B3)}$$

$$= \chi[\langle\hat{O}u_\alpha(k) | \hat{O}i\partial_k u_\beta(k)\rangle$$
$$+ (\partial_k\theta_\beta)\langle\hat{O}u_\alpha(k) | \hat{O}u_\beta(k)\rangle]e^{i(\theta_\alpha(k)-\theta_\beta(k))}. \quad \text{(B4)}$$

Here, $\hat{O} = \hat{\Pi}$ is a unitary operator and $\hat{O} = \hat{\Theta}, \hat{\Pi}\hat{\Theta}$ are antiunitary operators. These operators obey

$$\langle\hat{O}\psi | \hat{O}\phi\rangle = \begin{cases} \langle\psi | \phi\rangle & \text{if } \hat{O} \text{ is unitary (U)} \\ \langle\phi | \psi\rangle & \text{if } \hat{O} \text{ is antiunitary (A)} \end{cases} \quad \text{(B5)}$$

for arbitrary states $|\psi\rangle, |\phi\rangle$. Hereafter, we substitute (U), (A) for unitary or antiunitary $\hat{O}$, respectively.

Then, we find from Eq. (B4) that

$$A_{\tilde{\alpha}\tilde{\beta}}(\chi k) = \begin{cases} \chi[+A_{\alpha\beta}(k) + (\partial_k\theta_\beta)\delta_{\alpha\beta}]e^{i(\theta_\alpha(k)-\theta_\beta(k))} & \text{(U)} \\ \chi[-A^*_{\alpha\beta}(k) + (\partial_k\theta_\beta)\delta_{\alpha\beta}]e^{i(\theta_\alpha(k)-\theta_\beta(k))} & \text{(A)} \end{cases}. \quad \text{(B6)}$$

Furthermore, the shift vector $R_{\tilde{\alpha}\tilde{\beta}}(\chi k)$ $(\alpha \neq \beta)$ satisfies

$$R_{\tilde{\alpha}\tilde{\beta}}(\chi k)$$
$$= A_{\tilde{\alpha}\tilde{\alpha}}(\chi k) - A_{\tilde{\beta}\tilde{\beta}}(\chi k) - \partial_{\chi k}\arg A_{\tilde{\alpha}\tilde{\beta}}(\chi k) \quad \text{(B7)}$$

$$= \begin{cases} +\chi[A_{\alpha\alpha}(k) - A_{\beta\beta}(k) - \partial_k\arg A_{\alpha\beta}(k)](\text{U}) \\ -\chi[A_{\alpha\alpha}(k) - A_{\beta\beta}(k) - \partial_k\arg A_{\alpha\beta}(k)](\text{A}) \end{cases}. \quad \text{(B8)}$$

where $\theta_{\alpha,\beta}$ vanishes because of the gauge invariance of the shift vector.

From Eqs. (B6) and (B8), we find the following relations:

$$|A_{\tilde{\alpha}\tilde{\beta}}(\chi k)| = |A_{\alpha\beta}(k)| \quad (\alpha \neq \beta), \quad \text{(B9a)}$$

$$R_{\tilde{\alpha}\tilde{\beta}}(\chi k) = \begin{cases} +\chi R_{\alpha\beta}(k) & \text{(U)} \\ -\chi R_{\alpha\beta}(k) & \text{(A)} \end{cases}. \quad \text{(B9b)}$$

Let us now consider a PT-symmetric system. In this case, $\hat{O} = \hat{\Pi}\hat{\Theta}$ is antiunitary (A) and $\chi = +1$. If we take $\alpha, \beta = (n, \uparrow), (m, \uparrow)$, we then find $\tilde{\alpha}, \tilde{\beta} = (n, \downarrow), (m, \downarrow)$. Taking these into account, we immediately obtain Eqs. (15) from Eqs. (B9).

Similarly, in a system with both inversion and time-reversal symmetries, we obtain

$$|A^\sigma_{nm}(-k)| = |A^\sigma_{nm}(k)|, \quad R^\sigma_{nm}(-k) = -R^\sigma_{nm}(k), \quad \text{(B10a)}$$

from the inversion symmetry, and

$$|A^\uparrow_{nm}(-k)| = |A^\downarrow_{nm}(k)|, \quad R^\uparrow_{nm}(-k) = +R^\downarrow_{nm}(k) \quad \text{(B10b)}$$

from the time-reversal symmetry. Combining Eqs. (B10a) and (B10b), we get Eqs. (15) and (16).

APPENDIX C: REASON FOR TUNNELING CURRENT OSCILLATION

We consider the components of the Hamiltonian of the zigzag chain models shown in Eqs. (27) and (34). We find that in both models, $\hat{H}^\sigma(k_0(t))$ is time-periodic with period

$T = 2\pi\hbar/(e|E|a)$. In this case, Floquet theory [[34], Sec. 3.6] gives some conditions for $|\Psi^\sigma_{k_0}(t)\rangle$ as a solution of Eq. (3). Note that we also have to pay attention to conservation of probability $\langle\Psi^\sigma_{k_0}(t) | \Psi^\sigma_{k_0}(t)\rangle = 1$. Then, we obtain the expression

$$\left|\Psi^\sigma_{k_0}(t)\right\rangle = \sum_{\nu=1,2} b^\sigma_{\nu k_0} e^{-i\varepsilon^\sigma_\nu t/\hbar}\left|\Phi^\sigma_{\nu k_0}(t)\right\rangle. \quad \text{(C1)}$$

Here, $|\Phi^\sigma_{\nu k_0}(t)\rangle$ is a time-periodic state with period T, and the Floquet exponent $i\varepsilon^\sigma_\nu$ is imaginary. We also introduced the coefficients $b^\sigma_{\nu k_0}$. Note that ε^σ_ν is independent of k_0 because Eq. (3) shows that the difference in k_0 is reduced to the shift of the origin of time, which has no effect on the Floquet exponent of the solution.

Furthermore, when the system has time-reversal symmetry, ε^σ_ν is also independent of σ because the time-reversal operation (antiunitary) and the subsequent change of variable $t \to -t$ converts the Schrödinger equation (3) and the solution (C1) with the label (k_0, σ) into those with $(-k_0, -\sigma)$, but the Floquet exponent is unchanged.

Now, we find

$$\left\langle\Psi^\sigma_{k_0}(t)\right| \hat{H}^\sigma(k_0(t)) \left|\Psi^\sigma_{k_0}(t)\right\rangle$$
$$= \sum_{\mu,\nu} b^{\sigma*}_{\mu k_0} b^\sigma_{\nu k_0} e^{i(\varepsilon^\sigma_\mu - \varepsilon^\sigma_\nu)t/\hbar}\left\langle\Phi^\sigma_{\mu k_0}(t)\right| \hat{H}^\sigma(k_0(t))\left|\Phi^\sigma_{\nu k_0}(t)\right\rangle$$
$$= \mathcal{P}_0(t) + \mathcal{P}_1(t)\cos\left(\omega^\sigma_{12}t\right) + \mathcal{P}_2(t)\sin\left(\omega^\sigma_{12}t\right) \quad \text{(C2)}$$

where $\mathcal{P}_{0,1,2}(t)$ are all real periodic function with period T, and $\omega^\sigma_{12} \equiv |\varepsilon^\sigma_1 - \varepsilon^\sigma_2|/\hbar$. Thus, we get from Eq. (8) and Eq. (A3),

$$j^\sigma = \frac{1}{EL}\sum_{k_0\in\text{BZ}} \frac{\partial}{\partial t}\left\langle\Psi^\sigma_{k_0}(t)\right| \hat{H}^\sigma(k_0(t))\left|\Psi^\sigma_{k_0}(t)\right\rangle \quad \text{(C3)}$$

$$= \mathcal{Q}_0(t) + \mathcal{Q}_1(t)\cos\left(\omega^\sigma_{12}t\right) + \mathcal{Q}_2(t)\sin\left(\omega^\sigma_{12}t\right) \quad \text{(C4)}$$

where $\mathcal{Q}_{0,1,2}(t)$ are all periodic with period T and j^σ has no dc component. As we mentioned above, $\omega^\uparrow_{12} = \omega^\downarrow_{12}$ also holds in time-reversal symmetric systems.

APPENDIX D: APPROXIMATION OF TUNNELING CURRENT SHORTLY AFTER APPLICATION OF ELECTRIC FIELD

In the adiabatic limit, Eq. (14) leads to

$$\begin{pmatrix} a^\sigma_{+k_0}(t)e^{-i\arg A^\sigma_{+-}(k_0)} \\ a^\sigma_{-k_0}(t) \end{pmatrix} \simeq \left[\mathbb{1} + i\int_{-k_0}^{k_0(t)} |A^\sigma_{+-}(k)| \begin{pmatrix} 0 & e^{-i\Delta^\sigma_{+-}(k,k_0)} \\ e^{+i\Delta^\sigma_{+-}(k,k_0)} & 0 \end{pmatrix} dk\right]\begin{pmatrix} 0 \\ 1 \end{pmatrix}. \quad \text{(D1)}$$

For convenience, we write $A_0 \equiv |A^\sigma_{+-}|$, $R_0 \equiv R^\uparrow_{+-}$, $q \equiv -eEt/\hbar$ and $\lambda \equiv (\epsilon_{\text{gap}}/eE) + \sigma R_0$. We assume that t is small enough to satisfy $|q|a \ll 1$ where a is the lattice constant, hereafter taken as $a = 1$. We also consider the band parameter w shown in Eq. (28) as a typical energy scale, and set $w = 1$ for simplicity. By using the Taylor expansion with q, we find that

$$P^\sigma_{k_0}(E, t) = \left|a^\sigma_{+k_0}\right|^2 \quad \text{(D2)}$$

$$= \left| \int_{k_0}^{k_0+q} dk\, A_0 \exp\left(-i \int_{k_0}^{k} dk'\, \lambda\right) \right|^2 \tag{D3}$$

$$= \left| A_0(k_0)\frac{q^1}{1!} + (\partial_k - i\lambda)A_0\big|_{k=k_0}\frac{q^2}{2!} \right.$$

$$\left. + (\partial_k - i\lambda)^2 A_0\big|_{k=k_0}\frac{q^3}{3!} + (\partial_k - i\lambda)^3 A_0\big|_{k=k_0}\frac{q^4}{4!} + \cdots \right|^2 \tag{D4}$$

$$\equiv P_{k_0}^{\sigma}(E, q). \tag{D5}$$

The tunneling current Eq. (9) is expressed as

$$j^{\sigma} = \frac{-e}{\hbar} \int_{\text{BZ}} \frac{dk_0}{2\pi} \frac{\partial}{\partial q}\big[\epsilon_{\text{gap}}(k_0 + q)P_{k_0}^{\sigma}(E, q)\big]. \tag{D6}$$

We expand this formula with q by using Eq. (D5) and the expansion $\epsilon_{\text{gap}}(k_0 + q) = \epsilon_{\text{gap}}(k_0) + \partial_k \epsilon_{\text{gap}}|_{k=k_0} q^1/1! + \cdots$. Then, we find

$$\epsilon_{\text{gap}}(k_0 + q)P_{k_0}^{\sigma}(E, q)/q^2 = c_{0,0} + c_{1,0}q^1$$

$$+ [c_{2,2}(E/E_0)^{-2} + c_{2,1}(E/E_0)^{-1}\sigma + c_{2,0}]q^2$$

$$+ [c_{3,2}(E/E_0)^{-2} + c_{3,1}(E/E_0)^{-1}\sigma + c_{3,0}]q^3$$

$$+ \mathcal{O}((t/t_0)^4) \tag{D7}$$

where we introduced $E_0 = w/(ea)$ and $t_0 = \hbar/w$. The coefficients $c_{l,m}$ consist of ϵ_{gap}, A_0 and R_0, for example,

$$c_{0,0} = \epsilon_{\text{gap}}A_0^2\big|_{k=k_0}, \quad c_{2,1} = -\tfrac{1}{6}\epsilon_{\text{gap}}^2 A_0^2 R_0\big|_{k=k_0}, \tag{D8}$$

$$c_{3,1} = \frac{1}{12}\big[(\epsilon_{\text{gap}}(\partial_k \epsilon_{\text{gap}})A_0^2 R_0 - \partial_k(\epsilon_{\text{gap}}^2 A_0^2 R_0)\big]\big|_{k=k_0}. \tag{D9}$$

Then, the leading term of the charge current $j^{\text{c}} = j^{\uparrow} + j^{\downarrow}$ is given as follows:

$$j^{\text{c}}(E, t) \simeq 2\frac{-e}{\hbar} \int_{\text{BZ}} \frac{dk_0}{2\pi} c_{0,0} 2q^1 \tag{D10}$$

$$= -\frac{2}{\pi} j_0^{\text{c}} \left(\frac{1}{aw} \int_{\text{BZ}} dk\, \epsilon_{\text{gap}}A_0^2\right)\left(\frac{E}{E_0}\right)^1 \left(\frac{t}{t_0}\right)^1. \tag{D11}$$

Here, we reinserted the powers of a and w from dimensional analysis. The leading term of the spin current $j^{\text{s}} = (\hbar/2(-e))(j^{\uparrow} - j^{\downarrow})$ in a PT-symmetric system is also given as follows:

$$j^{\text{s}}(E, t) \simeq 2\frac{\hbar}{2(-e)}\frac{-e}{\hbar} \int_{\text{BZ}} \frac{dk_0}{2\pi} c_{2,1}\left(\frac{E}{E_0}\right)^{-1} 4q^3. \tag{D12}$$

This equation leads to Eq. (36).

However, in a system with both inversion and time-reversal symmetries, the integral in Eq. (D12) vanishes because the coefficient $c_{2,1}(k)$ is an odd function of k. In general, $c_{l,m}(-k_0) = (-1)^{l+m}c_{l,m}(k_0)$ holds because the expansion (D7) is valid regardless of the inversion transformation $(E, \sigma, q) \rightarrow (-E, +\sigma, -q)$. Therefore, the leading term of j^{s} in this system is given as

$$j^{\text{s}}(E, t) \simeq 2\frac{\hbar}{2(-e)}\frac{-e}{\hbar} \int_{\text{BZ}} \frac{dk_0}{2\pi} c_{3,1}\left(\frac{E}{E_0}\right)^{-1} 5q^4, \tag{D13}$$

which leads to Eq. (32).

[1] J. Fabian, A. Matos-Abiague, C. Ertler, P. Stano, and I. Žutić, Semiconductor spintronics, Acta Physica Slovaca **57**, 565 (2007).

[2] D. Culcer and R. Winkler, Generation of Spin Currents and Spin Densities in Systems with Reduced Symmetry, Phys. Rev. Lett. **99**, 226601 (2007).

[3] M. Seemann, D. Ködderitzsch, S. Wimmer, and H. Ebert, Symmetry-imposed shape of linear response tensors, Phys. Rev. B **92**, 155138 (2015).

[4] K. Hamamoto, M. Ezawa, K. W. Kim, T. Morimoto, and N. Nagaosa, Nonlinear spin current generation in noncentrosymmetric spin-orbit coupled systems, Phys. Rev. B **95**, 224430 (2017).

[5] S. Kitamura, N. Nagaosa, and T. Morimoto, Current response of nonequilibrium steady states in the Landau-Zener problem: Nonequilibrium Green's function approach, Phys. Rev. B **102**, 245141 (2020).

[6] S. Murakami, N. Nagaosa, and S.-C. Zhang, Dissipationless quantum spin current at room temperature, Science **301**, 1348 (2003).

[7] C. Zener, A theory of the electrical breakdown of solid dielectrics, Proc. R. Soc. London. Sec. A **145**, 523 (1934).

[8] L. D. Landau, Zur theorie der energieübertragung. II, Phys. Z. Sowjetunion **2**, 46 (1932).

[9] C. Zener, Non-adiabatic crossing of energy levels, Proc. R. Soc. London. Sec. A **137**, 696 (1932).

[10] L. D. Landau and E. M. Lifshitz, *Quantum Mechanics: Non-Relativistic Theory*, Course of Theoretical Physics (Elsevier, Amsterdam, 1981).

[11] Here, we can construct each of the 32 PT-symmetric point groups G as a set made up of all the symmetry operations of the ordinary crystallographic point group G_0 plus the product of those operations with PT operation $\Pi\Theta$, namely $G = G_0 + \Pi\Theta G_0$. There are 21 black-white groups in the 32 PT-symmetric point groups (listed in Refs. [[35], Table XXXVI] and [[36], Appendix C]), and the rest of the 11 are centrosymmetric gray groups (listed in Refs. [[3], Table I] and [[35], Table XXXVI], in the column "magnetic Laue group").

[12] The authors of Ref. [3] classified the tensor forms by the magnetic Laue group that is generated by adding the spatial inversion operation to the original magnetic point group. The magnetic Laue groups for the PT-symmetric point groups are equivalent to the 11 centrosymmetric gray groups, and are listed in Table I in their paper.

[13] X. Zhang, Q. Liu, J.-W. Luo, A. J. Freeman, and A. Zunger, Hidden spin polarization in inversion-symmetric bulk crystals, Nat. Phys. **10**, 387 (2014).

[14] L. Yuan, Q. Liu, X. Zhang, J.-W. Luo, S.-S. Li, and A. Zunger, Uncovering and tailoring hidden Rashba spin-orbit splitting in centrosymmetric crystals, Nat. Commun. **10**, 906 (2019).

[15] M. V. Berry, Geometric amplitude factors in adiabatic quantum transitions, Proc. R. Soc. London. Sec. A **430**, 405 (1990).

[16] S. Kitamura, N. Nagaosa, and T. Morimoto, Nonreciprocal Landau-Zener tunneling, Commun. Phys. **3**, 63 (2020).

[17] S. Takayoshi, J. Wu, and T. Oka, Nonadiabatic nonlinear optics and quantum geometry - Application to the twisted Schwinger effect, SciPost Phys. **11**, 075 (2021).

[18] J. E. Sipe and A. I. Shkrebtii, Second-order optical response in semiconductors, Phys. Rev. B **61**, 5337 (2000).

[19] S. M. Young and A. M. Rappe, First Principles Calculation of the Shift Current Photovoltaic Effect in Ferroelectrics, Phys. Rev. Lett. **109**, 116601 (2012).

[20] A. M. Cook, B. M. Fregoso, F. De Juan, S. Coh, and J. E. Moore, Design principles for shift current photovoltaics, Nat. Commun. **8**, 14176 (2017).

[21] T. Morimoto and N. Nagaosa, Topological nature of nonlinear optical effects in solids, Sci. Adv. **2**, e1501524 (2016).

[22] H. Kusunose, *Electron Theory of Spin–Orbit-Coupled Physics* (Kodansha Ltd., Tokyo, 2019).

[23] Y. Yanase, Magneto-electric effect in three-dimensional coupled zigzag chains, J. Phys. Soc. Jpn. **83**, 014703 (2014).

[24] Y. Sugita, S. Hayami, and Y. Motome, Antisymmetric spin-orbit coupling in a d-p model on a zigzag chain, Phys. Procedia **75**, 419 (2015).

[25] S. Hayami, H. Kusunose, and Y. Motome, Emergent spin-valley-orbital physics by spontaneous parity breaking, J. Phys.: Condens. Matter **28**, 395601 (2016).

[26] See Supplemental Material at http://link.aps.org/supplemental/10.1103/PhysRevB.105.075201 for additional numerical results for the zigzag chain models, including numerical accuracy regarding the conservation of probability, Fourier spectrum of the oscillating current, spin current dependence on the parameter v, and charge current dependence on electric field.

[27] S. Hayami, H. Kusunose, and Y. Motome, Spontaneous multipole ordering by local parity mixing, J. Phys. Soc. Jpn. **84**, 064717 (2015).

[28] T. Oka and H. Aoki, Ground-State Decay Rate for the Zener Breakdown in Band and Mott Insulators, Phys. Rev. Lett. **95**, 137601 (2005).

[29] H. Aoki, N. Tsuji, M. Eckstein, M. Kollar, T. Oka, and P. Werner, Nonequilibrium dynamical mean-field theory and its applications, Rev. Mod. Phys. **86**, 779 (2014).

[30] H. Xu, H. Wang, J. Zhou, and J. Li, Pure spin photocurrent in non-centrosymmetric crystals: Bulk spin photovoltaic effect, Nat. Commun. **12**, 4330 (2021).

[31] B. Göhler, V. Hamelbeck, T. Z. Markus, M. Kettner, G. F. Hanne, Z. Vager, R. Naaman, and H. Zacharias, Spin selectivity in electron transmission through self-assembled monolayers of double-stranded DNA, Science **331**, 894 (2011).

[32] Z. Xie, T. Z. Markus, S. R. Cohen, Z. Vager, R. Gutierrez, and R. Naaman, Spin specific electron conduction through DNA oligomers, Nano Lett. **11**, 4652 (2011).

[33] R. Naaman, Y. Paltiel, and D. H. Waldeck, Chiral molecules and the electron spin, Nat. Rev. Chem. **3**, 250 (2019).

[34] G. Teschl, *Ordinary Differential Equations and Dynamical Systems*, Graduate Studies in Mathematics Vol. 140 (American Mathematical Soc., Providence, Rhode Island, 2012).

[35] M. Yatsushiro, H. Kusunose, and S. Hayami, Multipole classification in 122 magnetic point groups for unified understanding of multiferroic responses and transport phenomena, Phys. Rev. B **104**, 054412 (2021).

[36] H. Watanabe and Y. Yanase, Chiral Photocurrent in Parity-Violating Magnet and Enhanced Response in Topological Antiferromagnet, Phys. Rev. X **11**, 011001 (2021).